

# Effects of enhanced surfaces and surface orientation on nucleate and film boiling heat transfer in R-11

D. S. JUNG†

Thermal Machinery Group, Center for Building Technology, National Bureau of Standards,  
Gaithersburg, MD 20899, U.S.A.

and

J. E. S. VENART and A. C. M. SOUSA

Mechanical Engineering Department, University of New Brunswick, Fredericton, NB, Canada E3B 5A3

(Received 2 December 1986 and in final form 11 May 1987)

**Abstract**—A study of pool boiling heat transfer in R-11 is reported as a function of surface characterization and orientation. Two specially prepared metal coated surfaces (UNB#1, UNB#2) and a flat copper surface were subjected to heat fluxes up to  $180 \text{ kW m}^{-2}$  with surface orientations varying from horizontally facing upward ( $0^\circ$ ), to vertical ( $90^\circ$ ), to horizontally facing downward ( $180^\circ$ ). The resulting nucleate boiling curves display considerable boiling hysteresis and enhanced surfaces show 2–3 times better heat transfer than a plain surface. Rohsenow's nucleate boiling equation is used to correlate the data and modified to account for the effects of surface characterization and orientation. In film boiling, enhanced surfaces also reveal better heat transfer characteristics and the role of surface orientation on the motion and stability of the vapor film is clarified.

## 1. INTRODUCTION

AS THE use of industrial fluids has increased rapidly, there have been a rising number of accidents of railroad tankcars or storage tanks carrying such hazardous fluids as propane, butadiene, ammonia, ethylene, and vinyl chloride. These accidents have caused death, serious injury, extensive property damage, and disruptive major evacuations [1]. When a tank is exposed to fire, heat is conducted through the tank wall and dissipated into the bulk liquid. At low heat flux, single phase natural convection is predominant and as the heat flux increases continuously, boiling takes place inside the tank resulting in a vigorous bubble formation on the wall as shown in Fig. 1. Tanks normally utilize large horizontal cylinders and hence the interior fluid sees a variety of surface orientations with respect to the gravitational field. In order to make the shipping and storage of the hazardous industrial fluids safer, enhanced surfaces have been proposed [1] as an internal protection device to keep tanks safe in case of external fire. With these enhanced surfaces, the tank wall temperature can be maintained sufficiently low due to their high heat transfer performance. The objectives of this study are to determine the nucleate and film boiling heat transfer performance of enhanced surfaces and compare it with that of a plain surface and to investigate the effect of surface orientation on pool boiling for design purposes. For the simplicity of the analysis, it is

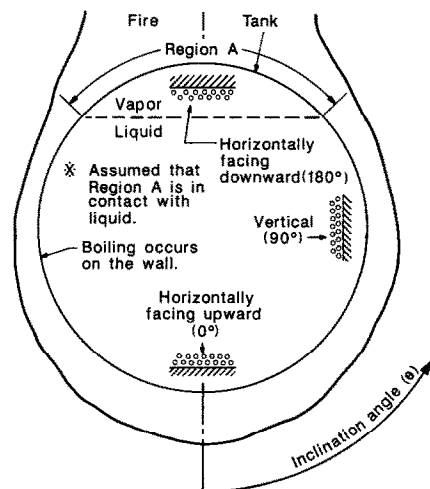


FIG. 1. Cross-sectional view of a horizontal tank engulfed by fire.

assumed that a tank engulfed by fire sits horizontally and is full of liquid as shown in Fig. 1.

Nucleate boiling heat transfer has been the subject of extensive studies during the past several decades owing to its effective heat transfer characteristics. Even though heat transfer coefficients for nucleate boiling are high, further improvements are often required especially in such fields as petrochemical processing, liquefaction, air separation, refrigeration, power plant, and electric equipment. The high cost of energy and heat transfer equipment has accelerated the development of techniques for enhancing heat transfer. Due to intensive studies during the last three

† Former Graduate Research Assistant at UNB, Canada.

## NOMENCLATURE

$a, b$	exponents in equation (1)	Greek symbols	
$C_1$	constants in equation (3)	$\theta$	inclination angle [deg]
$C_{sf}$	constant in equation (2)	$\mu$	viscosity [Pa s]
$C_p$	specific heat [ $\text{J kg}^{-1} \text{K}^{-1}$ ]	$\rho$	density [ $\text{kg m}^{-3}$ ]
$g$	acceleration of gravity [ $\text{m s}^{-2}$ ]	$\sigma$	surface tension [ $\text{N m}^{-1}$ ].
$h$	heat transfer coefficient [ $\text{W m}^{-2} \text{K}^{-1}$ ]	Subscripts	
$h_{fg}$	latent heat of vaporization [ $\text{J kg}^{-1}$ ]	est	estimated
$k$	thermal conductivity [ $\text{W m}^{-1} \text{K}^{-1}$ ]	hyd	hydrodynamically determined
$q$	heat flux [ $\text{kW m}^{-2}$ ]	min	minimum
$r, s$	exponents in equation (2)	Ro	roughness
$\Delta T$	superheat [K]	v	vapor
$\Delta x$	thickness [m].	l	liquid.

decades, a variety of methods has been proposed. Reviews of developments in augmented heat transfer are available elsewhere [2].

In boiling, of greatest interest are the special surfaces which promote nucleate boiling with a low wall superheat. One type of structured boiling surface is a metal coated porous surface produced by sintering or flame spraying. The objective of this surface treatment is to provide a larger number of active cavities which are stable with a lower wall superheat. The first study of this type of metal coated surfaces, known as a 'high flux' surface, was initiated in 1947 in an effort to reduce the wall superheat, pressure drop, size, and cost of heat exchangers in air separation plants [3]. O'Neill *et al.* [4] proposed the use of these 'high flux' surfaces to improve the overall heat transfer coefficient of heat exchangers in an LNG plant. They found the performance of the porous surface was stable with time and unaffected by light-fouling environments. Nishikawa *et al.* [5] performed boiling experiments in R-11 and R-113 with horizontal cylinders covered by a sintered layer of metal powder. They observed that the nucleate boiling heat transfer coefficients were dependent upon the thickness and thermal conductivity of the sintered layer. Yilmaz *et al.* [6], and Marto and Lepere [7] compared the nucleate boiling heat transfer performance of a 13 mm o.d. plain copper tube with three commercially available enhanced tubes: a Wieland Gewa-T tube, a Hitachi thermoexcel-E tube, and a Union Carbide High Heat Flux tube. They found that the Union Carbide High Heat Flux tube, manufactured by depositing metal particles on a tube, was superior to the other two commercial tubes which had uniform nucleation sites formed by deforming the original plain surface. Recently, Bergles and Chyu [8] conducted nucleate boiling experiments in both distilled water and R-113 using a 25 mm o.d. plain copper tube and three different Union Carbide High Heat Flux tubes. They investigated the effects of surface structure, boiling liquid, surface aging, and surface sub-

cooling. They observed that the heat transfer coefficients for porous boiling surfaces were 2.5 times higher than those for a plain surface.

Film boiling heat transfer has got relatively less attention due to its lower heat transfer capability as compared to that of nucleate boiling heat transfer. As modern techniques are developed in such fields as nuclear reactors and space technologies, a knowledge about the conditions necessary to sustain film boiling such as the minimum temperature difference,  $(\Delta T)_{\min}$ , and minimum heat flux,  $q_{\min}$ , is essential. When equipment must be operated in the film boiling regime, which is quite often encountered in cryogenics, a knowledge of  $(\Delta T)_{\min}$  and  $q_{\min}$  is very important for design purposes. Film boiling is characterized by a thin vapor film which separates the bulk liquid from the heating surface. Since Bromley's [9] pioneering work in 1950, Chang [10] and Zuber [11] studied the hydrodynamic aspects of film boiling. Berenson [12] succeeded in predicting film boiling heat transfer using Taylor's instability theory and derived a functionality between the heat transfer coefficient and minimum superheat. In the subsequent work, Berenson [13] observed that the surface finish on plain surfaces neither affected the film boiling data nor changed the minimum temperature difference. Hosler and Westwater [14] compared Berenson's model with their experimental data obtained in R-11 and concluded that his method for predicting the film boiling curve was good but the prediction of the minimum temperature difference was not reliable.

The effect of surface orientation in nucleate boiling was reported by Githinji and Sabersky [15] in 1963. They made comparisons of boiling heat transfer from a 0.3 cm wide strip in isopropyl alcohol for three different surface orientations: horizontally facing upward, vertical, and horizontally facing downward. They observed that the boiling curve for the horizontal strip facing downward differed significantly from those for the other orientations. Recently Chen [16] conducted similar pool boiling experiments in R-

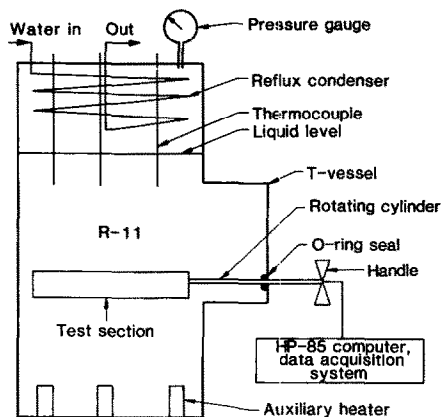


FIG. 2. Schematic diagram of experimental apparatus.

11 using a  $3.7 \times 2.5$  cm copper plate. He concluded that the heat transfer coefficient at a given wall superheat increased as the inclination angle increased from  $0^\circ$  (horizontally facing upward) to about  $150^\circ$  (inclined facing downward  $30^\circ$ ) and dropped rapidly to a minimum value at  $180^\circ$  (horizontally facing downward). Seki *et al.* [17] performed film boiling experiments in R-11 for the cases when the horizontal plate was facing up ( $0^\circ$ ) and down ( $180^\circ$ ). They observed that the vapor motion on the heating surface was a strong function of surface orientation in film boiling. They also pointed out that the heat transfer coefficient for the horizontal plate facing upward was several times higher than that for the horizontal plate facing downward in film boiling.

To the authors' knowledge, there has not been any work reported regarding the surface orientation effect with enhanced surface on nucleate and film boiling heat transfer.

## 2. EXPERIMENTS

### 2.1. Experimental apparatus

A schematic diagram of the apparatus is presented in Fig. 2. A pyrex glass vessel with a T-section (43 cm tall, 15 cm diameter at both ends, 10 cm diameter at T-section) was used as a pool. Two plexiglas end plates and an aluminum plate (28 cm diameter, 2.5 cm thick) served as covers for the top, side, and bottom of the pool, respectively. O-Rings were used for sealing between the covers and the glass vessel. As a working fluid, R-11 was used throughout the experiments. The vapor generated was condensed by a reflux condenser made of a 1 cm o.d. copper tube and suspended from the top plexiglas cover. To bring the system pressure to a desired level, three auxiliary heaters in aluminum holders were installed on the bottom aluminum plate. A stainless steel tube (1 cm o.d., 25 cm long) was used as a rotating cylinder on which a protractor and an indicator for surface orientation were fixed. This tube also contained power and thermocouple leads from the heater, which were connected to a HP-85 computer and data acquisition system as shown in Fig. 2. The

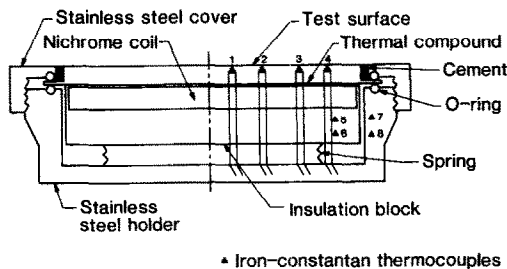


FIG. 3. Detailed cross-sectional view of test section.

heating test section could be easily rotated to a desired surface orientation by turning a handle fixed on the rotating cylinder.

A detailed cross-sectional view of the heater is given in Fig. 3. Two types of flat 7.8 cm diameter test surfaces were used: a plain surface made of copper and two enhanced surfaces (UNB #1, UNB #2). While the plain copper surface was prepared by polishing with a coarse emery paper, the enhanced surfaces were manufactured by depositing metal particles on plain mild steel plates. This metal coating process requires the application of metal powder to a workpiece by means of a torch especially developed for this purpose. The torch burns out a conventional oxyacetylene mixture and the powder. A fine mesh surfacing alloy is swept along by the force of the gas and is sprayed onto the workpiece while it melts. The detailed manufacturing process for UNB #1 and UNB #2 is available elsewhere [18]. A threaded stainless steel container with an easily removable cover was made to facilitate the replacement of the test surface with another and to hold the heating element in place. The heating element was composed of two parts. One was a nichrome coil used to achieve a uniform temperature distribution on the heating surface. The other was an insulation block made of a machinable ceramic, serving as a housing for the nichrome coil as well as limiting the heat transfer to the surface. A very thin thermally good conductive compound was applied in between the test surface and heating element for a good thermal contact. The heating element was spring-loaded for better heat transfer.

Eight 30 gage iron-constantan thermocouples were used to measure the temperatures on the surface, insulation block, and stainless steel holder as shown in Fig. 3. Four holes were drilled just underneath the surface and through the insulation block to mount thermocouples. The temperatures in the insulation block and stainless steel holder were used for the heat loss calculation through the bottom and circumference of the insulation block. Three 30 gage copper-constantan thermocouples were immersed in the pool to measure the bulk temperature as shown in Fig. 2. The accuracy of the temperature measurements was typically  $\pm 0.1^\circ\text{C}$ . Three temperatures in the pool differed from each other by  $0.1$ – $0.15^\circ\text{C}$  indicating that the pool was fairly isothermal. For the pressure measurement, a calibrated pressure gage was installed on the top plexiglas end plate. The accuracy of the

pressure measurement is within 1.5% of the reading. Even though the glass vessel was insulated, a sub-cooling of 0.5–1°C was observed throughout the tests.

## 2.2. Experimental procedure

For nucleate boiling tests the experimental procedure for an individual run consists of the following steps.

- (1) The heat transfer surface is cleaned with acetone before testing.
- (2) The working fluid is charged and preheated to bring the system up to the desired pressure and subsequently degassed.
- (3) Power to the main heater is initiated for the plate facing upward.
- (4) When the system reaches steady state, data for the present orientation is obtained.
- (5) With the same heat flux, the surface orientation is changed to the next desired one. Throughout the tests, the orientations at which data is taken are 0°, 45°, 90°, 135°, 150°, 160°, 170°, and 180°.
- (6) After data for all prespecified angles is obtained, the power level is increased.

An ordinary technique of obtaining film boiling, i.e. traversing up the nucleate boiling curve and over the peak heat flux, may require complex and high-capacity equipment, while the region of interest requires only a small fraction of the peak heat flux. Another vital drawback of this technique is that there is a strong possibility of heater burn out. In order to operate experiments in a safe manner, the observations made by Seki *et al.* [17] were utilized. As mentioned earlier in the paper, the peak heat flux for the horizontal plate facing downward (180°) is several times lower than that for the horizontal plate facing upward (0°) and hence it is easy and safe to establish film boiling from a horizontal surface facing downward at low heat flux. By taking advantage of this fact, the following steps are taken to obtain the data in film boiling.

- (1) Film boiling is established for the horizontal surface facing downward at low heat flux.
- (2) The rotating cylinder is turned to a desired surface orientation, maintaining a sufficient heat flux to sustain the film boiling by adjusting the power input to the main heater.
- (3) When the system reaches steady state, data for the present orientation is obtained.
- (4) The power input to the main heater is varied to obtain several data points including the minimum heat flux for the present orientation.
- (5) The surface orientation is changed to the next desired one and step (4) is repeated.

## 2.3. Data collection and reduction

Monitoring of eleven thermocouples and two a.c. voltage drops across the main heater and a standard resistor was done by using a HP-85 computer and

data acquisition system. It usually took 30 min for the system to reach steady state. The following items were stored for each steady-state data point: two a.c. voltages, four surface temperatures, three liquid temperatures, two temperatures in the insulation block, and two in the stainless steel holder. The standard deviation of the temperature measurements was 0.02–0.05°C. The power input to the main heater was calculated by using the two a.c. voltage drops. The heat flux associated with the boiling was subsequently obtained by subtracting the heat loss through the insulation block from the total heat input. In the heat loss calculation, one-dimensional heat conduction was assumed both axially and radially in the insulation block. The maximum error in the evaluated heat flux was estimated to be less than 3.5%. Detailed information is available in ref. [18]. Actual surface temperatures were calculated from the measured ones by using the one-dimensional heat conduction equation to account for the small temperature drop between the thermocouple location and the heating surface. The superheat,  $\Delta T$ , was then calculated by taking the difference between the averaged surface and bulk temperatures.

## 3. RESULTS AND DISCUSSION

### 3.1. Nucleate boiling

Figures 4–6 illustrate the nucleate boiling heat transfer results for the copper, UNB # 1, and UNB # 2 surfaces at 2 bar, respectively. These figures also include the free convection prediction curve of Fujii and Imura [19] for a plain horizontal plate facing upward at 2 bar for illustration.

3.1.1. *Effect of enhanced surfaces.* All surfaces show the existence of incipient boiling points, which marks the knee on the boiling curves as shown in Figs. 4–6. When the level of the superheat required for incipient boiling is reached, any small increase in the heat input results in a vigorous boiling accompanied by a sudden temperature drop of the surface. This effect is well

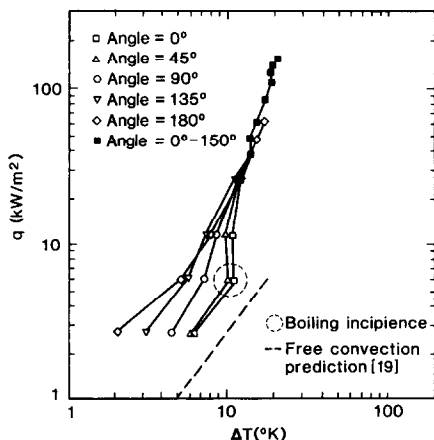


FIG. 4. Nucleate boiling heat transfer results for copper surface in R-11 at 2 bar.

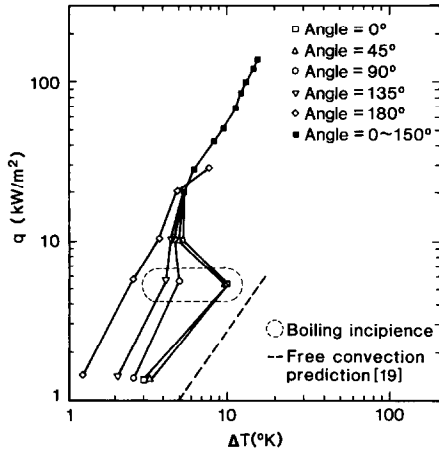


FIG. 5. Nucleate boiling heat transfer results for UNB #1 surface in R-11 at 2 bar.

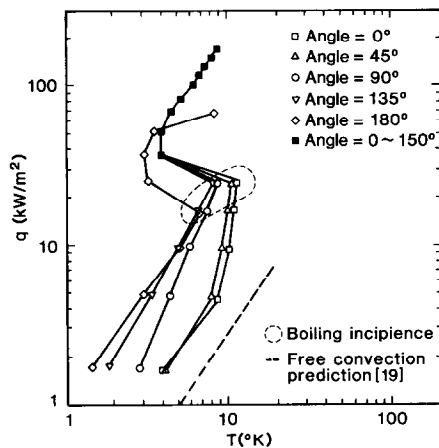


FIG. 6. Nucleate boiling heat transfer results for UNB #2 surface in R-11 at 2 bar.

illustrated in Fig. 7 which includes the boiling curves for the various surfaces facing upward at 2 bar. Heat flux is increased from the lowest data point to the highest one and then decreased to the lowest one. These are represented as the 'q increase' and 'q decrease', respectively, in Fig. 7. In the q increase, each surface shows a knee on the curve as mentioned earlier. On the other hand, in the q decrease, two distinct effects are observed. Firstly, the wall superheat continues to decrease with a progressive decrease in heat flux, which avoids the knee on the boiling curves. Secondly, for the heat flux range below the incipient boiling, the wall superheat is much smaller than that for the q increase. These results illustrate the effect of past history or 'hysteresis'. This effect results from the activation of nucleation sites as the heat flux decreases which had been inactive while the heat flux increased from a low value. In general, the enhanced surfaces are characterized by larger scale boiling hysteresis than the plain surface as shown in Fig. 7. Photographic studies of cross sections of the various surfaces were undertaken in an attempt to explain the large-scale hysteresis associated with the enhanced

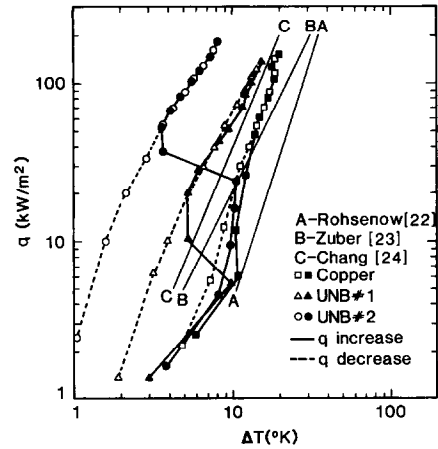


FIG. 7. Hysteresis effect on nucleate boiling for various horizontal surfaces facing upward and comparison of present results with theoretical predictions of nucleate boiling at 2 bar.

surfaces. As seen in Fig. 8, the heating surfaces used in this study are characterized as follows.

- (1) The plain copper surface does not have artificial pores except its own pits and scratches.
- (2) The UNB #1 surface has a number of large pores inside the metal coating.
- (3) The UNB #2 surface has a number of inter-connecting channels.

Due to the high wettability of R-11, typical contact angle of  $5^\circ$  [8] with copper, large pores and channels are easily flooded with liquid in the initial stage. Therefore, the metal coating is not sufficiently superheated to generate bubbles on its surface. Especially, the UNB #2 surface is harder for the metal coating to be activated as compared to the UNB #1 surface because of a shortage of non-wetted pores which act as re-entrant cavities to insure boiling at lower heat flux. In general, however, once the superheat becomes high enough to cause the metal coating to be activated, then the enhanced surfaces with high porosity undergo a vigorous boiling to reduce the superheat substantially while the plain surface is still in a weak boiling stage due to the lack of re-entrant cavities. This is the reason for the larger knees or temperature overshoots observed with the enhanced surfaces. The hysteresis effect is not important for most heat-exchanger applications in which operating heat fluxes are sufficient to cause the fully developed boiling immediately. However, this effect must be considered carefully in the applications where the heat flux is comparatively low in order to overcome the temperature overshoot.

As also illustrated in Fig. 7, the boiling curves for the enhanced surfaces are shifted to the left indicating that these surfaces have higher heat transfer coefficients than the plain surface. In the fully developed boiling regime, the best performance is shown by the UNB #2 surface showing 2–3 times heat transfer enhancement at constant heat flux as compared to a plain surface. On the other hand, the

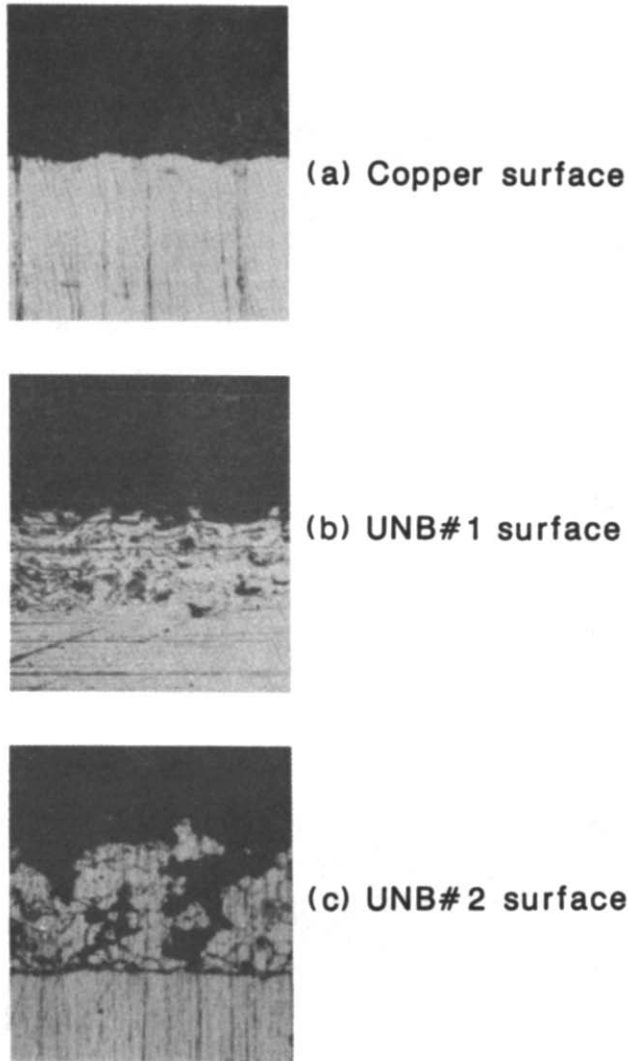


FIG. 8. Microscopic view of cross sections for various surfaces (100 $\times$ ).

UNB#1 surface shows 1.5–2 times enhancement. These heat transfer improvements may be explained by surface roughness test results obtained using a Talysurf 5 system. Figure 9 illustrates the typical surface profiles for the specimens. The UNB#2 records the highest surface roughness which is 7 times higher than that of the plain copper surface. The UNB#1 surface has a smaller value of surface roughness as compared to the UNB#2 surface but is still 4 times rougher than the copper surface. The nucleate boiling heat transfer results and surface roughness test results of the three specimens coincide very well with the previous investigations by Corty and Foust [20] who claimed that the rougher the surface, the better the heat transfer. The effect of surface roughness on boiling may be explained in the following fashion. In terms of the slope of the surface profile, the two enhanced surfaces have relatively higher values compared to the copper surface. The average slope inherently represents the ratio of the actual profile length

to the nominal profile length. The steeper the slope of the profile, the longer the actual length with its nominal length. Increase in actual length means that a surface has a larger actual heat transfer area which potentially provides higher site density or number of active sites per unit area. As Yamagata *et al.* [21] have shown by the correlation

$$q \sim (\Delta T)^a n^b \quad (1)$$

where  $n$  is the site density, the heat flux is proportional to the site density of a surface. It is believed from these results that the increase in site density is one of the reasons for the heat transfer improvements with the enhanced surfaces.

3.1.2. *Effect of surface orientation.* The effect of surface orientation is examined for all surfaces. Figures 10 and 11 illustrate the results. In the nucleate boiling regime for all surfaces, the superheat decreases by 15–25% as the inclination angle changes from 0° to 165° in the heat flux range 10–40 kW m<sup>-2</sup>. Beyond

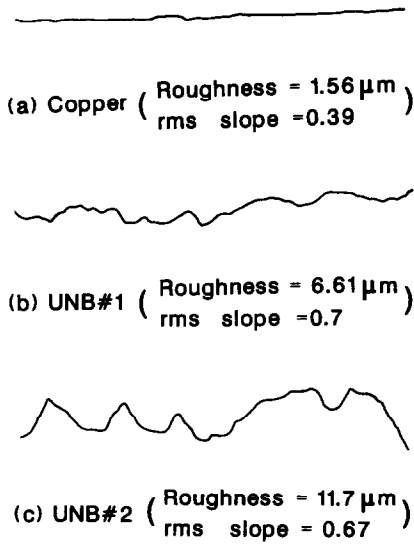


FIG. 9. Surface profiles and roughness values obtained with a Talysurf 5 system (horizontal distance = 0.2 mm, vertical distance = 0.1 mm).

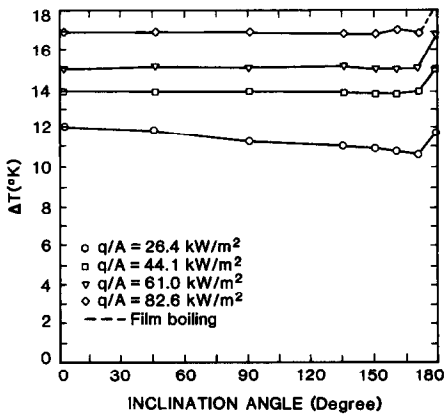


FIG. 10. Surface orientation effect on nucleate boiling heat transfer for copper surface in R-11 at 2 bar.

this heat flux, however, the superheat remains constant regardless of the surface orientation except for the horizontally facing downward case. This indicates that there are at least two types of heat transfer mechanism associated with nucleate boiling for the inclined surfaces. One is the evaporative mechanism which is always present regardless of the surface orientation and is dependent upon the heat flux. The other is the bubble agitation mechanism which is a strong function of the surface orientation. As the surface is inclined, there is a bubble flow over the surface which causes the surrounding fluid to be more turbulent resulting in an enhanced convection. At low heat flux the intensity of the evaporation is weak and the latter plays a relatively important role to take the heat away from the surface. At high heat flux, however, the evaporation mechanism is dominant and hence the latter effect becomes minimal. For the surfaces horizontally facing downward, the superheat required rises sub-

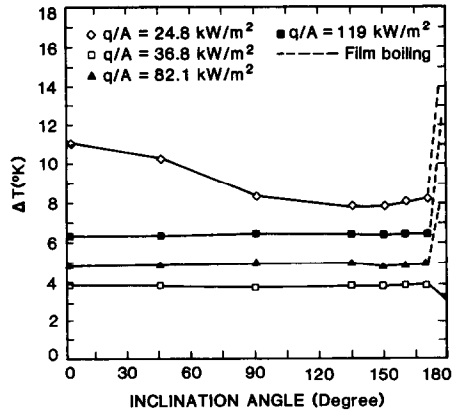


FIG. 11. Surface orientation effect on nucleate boiling heat transfer for UNB#2 surface in R-11 at 2 bar.

stantially showing the poorest heat transfer as shown in Figs. 10 and 11. This is explained by the fact that when the surface is horizontally facing downward, bubbles coalesce underneath the surface due to buoyancy force and gross convection currents are not sufficient to sweep bubbles away. As a consequence, the bubble motion does not add to the convection mechanism as it does when the surface is in other orientations. As the heat flux increases further, film boiling is observed much more easily at this orientation than at any other.

3.1.3. *Correlation.* Nucleate boiling heat transfer results for the various horizontal surfaces facing upward at 2 bar are compared with the theoretical predictions as shown in Fig. 7. None of the three well-known boiling equations correlates the data for the plain copper surface. This fact supports the premise of Rohsenow [22] that any boiling correlation which embodies only liquid and vapor properties of the working fluid cannot be a universal one. Besides, those correlations in Fig. 7 are no longer adequate to correlate the data for the enhanced surfaces since the correlations are derived on the basis of plain surfaces. Boiling curves are also shown to be a function of the surface orientation. From these considerations, it seems appropriate that some modifications are necessary in nucleate boiling correlations to account for the surface characteristics as well as orientation. Zuber and Forster's [23] and Chang and Snyder's [24] correlations have fixed constants and exponents so that there is no room for modification. This, however, is not the case with Rohsenow's [22] correlation. It has the unique flexibility that the constant ' $C_{sf}$ ' and the exponent ' $r$ ' in equation (2) can be changed according to the surface characteristics, surface-liquid combination and surface orientation, which was supported by Chen [16] and Vachon *et al.* [25]

$$\frac{C_{p1}\Delta T}{h_{fg}} = C_{sf} \left( \frac{q}{\mu_1 h_{fg}} \sqrt{\left( \frac{\sigma}{g(\rho_1 - \rho_v)} \right)} \right)^r \left( \frac{C_{p1}\mu_1}{k_1} \right)^s \quad (2)$$

Even though Rohsenow originally used 0.01, 0.33, and 1.7 for  $C_{sf}$ ,  $r$ , and  $s$ , respectively, he indicated that

Table 1. Physical properties of R-11 (from ref. [26])

Physical property	Unit	1 bar	2 bar
Liquid density	kg m <sup>-3</sup>	1479	1425
Vapor density	kg m <sup>-3</sup>	5.87	11.21
Liquid specific heat	J kg <sup>-1</sup> °C <sup>-1</sup>	870	892
Heat of evaporation	kJ kg <sup>-1</sup>	180	172
Liquid thermal conductivity	W m <sup>-1</sup> °C <sup>-1</sup>	8.65 × 10 <sup>-2</sup>	7.9 × 10 <sup>-2</sup>
Liquid viscosity	Pa s	4.27 × 10 <sup>-4</sup>	3.6 × 10 <sup>-4</sup>
Surface tension	N m <sup>-1</sup>	1.9 × 10 <sup>-2</sup>	1.58 × 10 <sup>-2</sup>

as a minimum the coefficient and even the exponent must change in magnitude as the surface-liquid combination and surface characteristics change. Based on this argument, the constant  $C_{sf}$  and exponent  $r$  in equation (2) are evaluated from the experimental data for the various surfaces at different orientations by using a least square method. Physical properties needed are from ref. [26] and shown in Table 1 and exponent  $s$  is set to 1.7. The correlation coefficient obtained from the reduction of the data is typically 0.96–0.98. Figure 12 shows the variation of  $C_{sf}$  and  $r$  as a function of the surface orientation at 2 bar. For the plain copper surface, as the surface inclination angle changes from 0° to 165°, exponent  $r$  increases by 40% and constant  $C_{sf}$  decreases a little bit and these two values jump to the higher values near 180°. Regarding the enhanced surfaces, they usually show two times higher  $r$  values than those of the plain surface. The enhanced surfaces, however, have 1.5–2 times lower values of  $C_{sf}$  as compared to the plain surface. These results exhibit that a surface treatment is one of the vital parameters in pool boiling correlation. Surface orientation, however, does not play an important role for the enhanced surfaces as it does for the plain surface. The values of  $r$  and  $C_{sf}$  remain constant regardless of the surface orientation except for the horizontal plate facing downward where both values again jump to higher values.

The present results for the plain horizontal copper surface facing upward (0°) at 2 bar are compared to Stephan and Abdelsalam's [27] correlation to see its

reliability in comparison with the existing experimental data in the literature. They applied the methods of regression analysis to nearly 5000 existing experimental data points to establish correlations for nucleate boiling. For refrigerants, they proposed the following equation for plain horizontal surfaces facing upward

$$h = C_1(\dot{q})^{0.745} \tag{3}$$

where  $h$ ,  $C_1$ , and  $\dot{q}$  are the heat transfer coefficient, a constant determined from properties (1.1 for R-11 at 2 bar), and heat flux in W m<sup>-2</sup>, respectively.

Equation (3) is changed by substituting the following relations:

$$h = \dot{q}/\Delta T \tag{4}$$

$$\dot{q} = 1000q \tag{5}$$

and rearranged as

$$q = 0.001453 (\Delta T)^{3.921} \tag{6}$$

where  $q$  is heat flux in kW m<sup>-2</sup>.

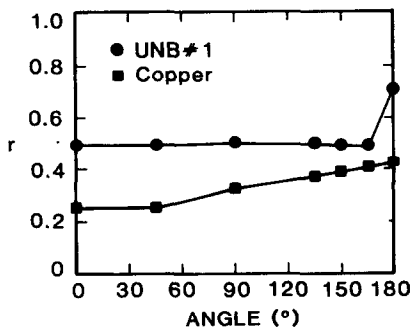
For the plain copper surface facing upward, Rohsenow's correlation with the constant  $C_{sf}$  and  $r$  shown in Fig. 12 turns out to be the following equation after all properties are substituted:

$$q = 0.001509 (\Delta T)^{3.893} \tag{7}$$

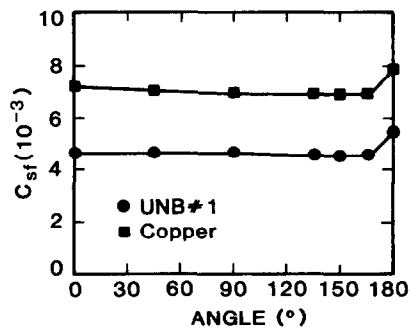
The constant and exponent in equation (7) differ by only 3.5 and 0.7% from the ones of equation (6), implying that the present result is in good agreement with the other experimental data in the literature. Based on the reliability of the present data, the following equations are proposed to account for the variation of  $C_{sf}$  and  $r$  in Rohsenow's correlation due to surface orientation for the plain surface.

For the plain inclined surface in the range of 0° to 150°

$$r = 0.256 - 1.514 \times 10^{-4}\theta + 1.778 \times 10^{-5}\theta^2 - 7.16 \times 10^{-8}\theta^3 \tag{8}$$



(a) Variation of 'r'



(b) Variation of 'C<sub>sf</sub>'

FIG. 12. Variation of  $r$  and  $C_{sf}$  in Rohsenow's correlation as a function of surface orientation at 2 bar.



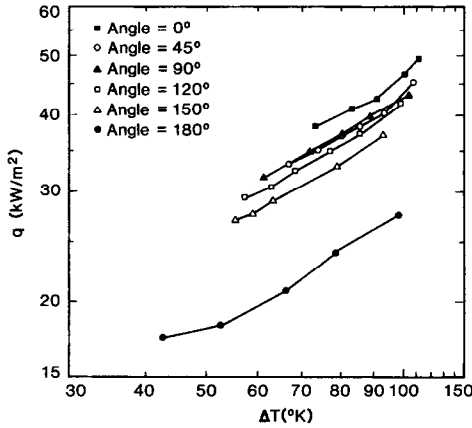


FIG. 13. Film boiling heat transfer results for copper surface in R-11 at 2 bar.

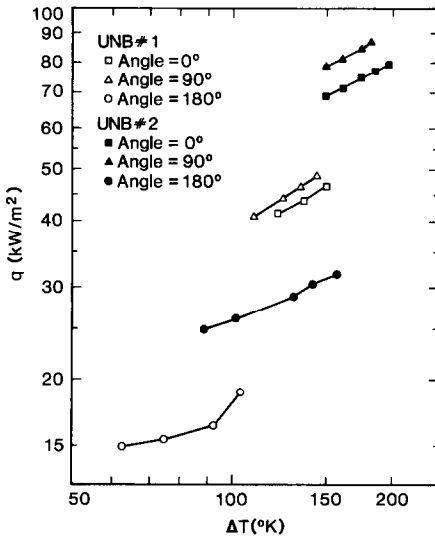


FIG. 14. Film boiling heat transfer results for enhanced surfaces in R-11 at 2 bar.

$$C_{sf} = 7.218 \times 10^{-3} - 1.74 \times 10^{-6}\theta \quad (9)$$

where  $\theta$  is the inclination angle in degrees.

### 3.2. Film boiling

Figures 13 and 14 and Table 2 show the film boiling test results for the various surfaces at 2 bar. Film boiling data could have been obtained at higher heat fluxes but only a few points including the minimum heat flux were taken for a given surface orientation since the minimum heat flux and corresponding minimum temperature difference were to be determined as precisely as possible at different surface orientations. A fouling reported by Akagawal *et al.* [28] was also observed at high heat flux in film boiling and this type of surface contamination wanted to be avoided.

The effect of surface orientation for the copper surface in film boiling is well illustrated in Fig. 13. As the inclination angle increases, two distinct points are observed. One is the superheat required increases accordingly for a given heat flux. The other is the

Table 2. Variation of  $q_{\min}$  and  $(\Delta T)_{\min}$  as a function of surface orientation for various surfaces in R-11 at 2 bar

	Angle (deg.)	$q_{\min}$ ( $\text{kW m}^{-2}$ )	$(\Delta T)_{\min}$ (K)
Copper	0	38.4	72.8
	45	33.2	66.7
	90	31.7	61.3
	120	29.6	56.8
	150	27.2	55.1
	180	17.7	42.6
UNB # 1	0	41.4	123.1
	90	41.1	110.0
	180	15.0	63.0
UNB # 2	0	68.8	151.9
	90	78.6	153.4
	180	24.9	89.4

minimum heat flux,  $q_{\min}$ , and minimum temperature difference,  $(\Delta T)_{\min}$ , diminish continuously as illustrated in Table 2 and Fig. 13. Except for the curve for the horizontally facing downward case all curves are located close together, leaving the curve for 180° much further below. This fact implies that there is a distinct difference in heat transfer between the horizontally facing downward case and other orientations in film boiling. The above-mentioned phenomena regarding the effect of orientation in film boiling can be explained by the consideration of the vapor motion and film thickness on the heating surface. Figure 15 illustrates how the vapor flow direction and buoyancy force affect the film boiling characteristics when the heating surface is inclined. For the horizontally upward facing case ( $0^\circ$ ) as shown in Fig. 15(b), the buoyancy force acts vertically to break off the vapor film vigorously and keep it unstable. Therefore, the frequency of the liquid contacting to the heating surface becomes higher. On the other hand, as for the facing upward inclined surface, shown in Fig. 15(a), vapor flows along the surface and breaks off at the trailing edge. Consequently, the thickness of the vapor film at the upper part of the surface will increase with the average film thickness greater than that for the

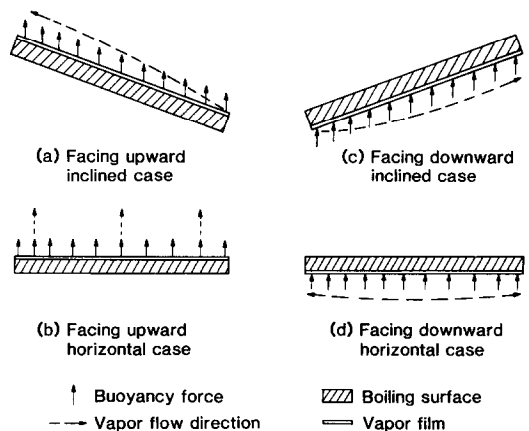


FIG. 15. Effect of buoyancy force and vapor flow direction on film boiling heat transfer.

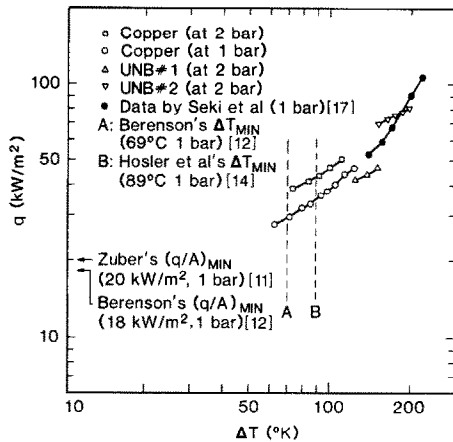


FIG. 16. Comparison of film boiling heat transfer results for horizontal copper surface facing upward with previous experimental data and theoretical predictions at 1 and 2 bar.

Table 3. Comparison of experimental data and theoretical prediction of film boiling heat transfer for horizontal copper surface facing upward at 1 bar

Investigator		$q_{\min}$ (kW m <sup>-2</sup> )	$(\Delta T)_{\min}$ (K)
Experimental data	Present result	27.6	63
	Seki <i>et al.</i> [17]	52	143
	Hosler and Westwater [14]	18	88.9
Theoretical prediction	Berenson [12]	18	69
	Zuber [11]	20	

horizontal facing upward case. The facing downward inclined case, as shown in Fig. 15(c), is similar to the facing upward inclined case except that this time buoyancy force acts toward the heating surface to stabilize the film and hence liquid access becomes more difficult causing poorer heat transfer. For the horizontally facing downward case (180°), however, there is a very stable vapor film covering the whole surface, which cuts the heat flow to the bulk liquid substantially. That is why this case showed the poorest heat transfer. From these considerations, it is evident that the motion and stability of the vapor film is strongly dependent upon the surface orientation and these factors are responsible for the variation of the film boiling data for the inclined surfaces. Enhanced surfaces also exhibited similar characteristics as shown in Fig. 14.

The present results for the horizontal copper surface facing upward (0°) at 1 bar are compared to the available experimental data and predictions as shown in Fig. 16 and Table 3. The minimum heat flux seems to exist with a  $\Delta T$  of 63 K within 10% deviation at 1 bar. However, this is not in good agreement with the previous investigations by Seki *et al.* (143 K) [17] and Hosler and Westwater (89 K) [14] as illustrated in Table 3. The discrepancy can be explained as follows: Seki *et al.* did not obtain the actual  $(\Delta T)_{\min}$ , whereas they simply extrapolated the nucleate and film boiling

Table 4. Comparison of various parameters for three horizontal surfaces facing downward at 2 bar

Parameter	Unit	Copper	UNB#1	UNB#2
Roughness	$\mu\text{m}$	1.56	6.61	11.7
$q_{\min}$	kW m <sup>-2</sup>	17.7	15.0	24.9
$(\Delta T)_{\min}$	K	42.6	63.0	89.4
$(\Delta T)_{R_o}$	K	3.26	11.66	34.41
$(\Delta T)_{\text{est}}$	K		51.0	73.0
$(\Delta T)_{\min} - (\Delta T)_{R_o}$	K	39.34	42.3	55.0

curves admitting that their data at the minimum heat flux was not reliable. However, if their curve is extended to a lower heat flux range, it would exactly coincide with the present results as shown in Fig. 16. As for Hosler and Westwater's results, their experimental apparatus did not permit operation at a  $\Delta T = 70$  K and they believed the  $(\Delta T)_{\min}$  to be less than their value. From these results, the minimum temperature difference in R-11 for the horizontal copper surface facing upward at 1 bar is believed to be 63 K. Berenson's prediction for the minimum superheat turns out to be quite accurate within 10% deviation from the present data for the horizontal plain surface facing upward. Theoretically predicted minimum heat fluxes, however, are 30% smaller than the present experimental data as shown in Table 3. These predictions could be used only to tell the lower bounds for the minimum heat flux.

Figure 16 also shows that there are large variations of the  $(\Delta T)_{\min}$  for the various surfaces at 2 bar. UNB#2 shows the largest value (152 K), UNB#1 next (123 K), and the copper surface has the smallest value (73 K). This fact is very much contradictory to Berenson's [13] experimental results obtained from plain surfaces with a different finish claiming that the minimum superheat is independent of the surface finish. Surface roughness test results are combined with the experimentally determined  $(\Delta T)_{\min}$  values in an attempt to explain the discrepancy between Berenson's and the present results. This ends up with the fact that the rougher the surface, the higher the minimum temperature difference,  $(\Delta T)_{\min}$ , as shown in Table 4. To examine the role of the surface roughness on  $(\Delta T)_{\min}$ , a simple one-dimensional heat flow analysis is done. For instance, one may assume that for the horizontal plain copper surface facing downward (180°) in which the vapor film is very stable as discussed earlier, the  $(\Delta T)_{\min}$  is composed of two parts. One is a  $(\Delta T)_{\text{hyd}}$  which is determined by the hydrodynamics of the fluid and assumed to be constant regardless of the surface roughness as long as the liquid level is kept constant. The other is a  $(\Delta T)_{R_o}$  which is the superheat drop across the minimum film thickness which is presumed to be equivalent to the surface roughness. The analysis is straightforward. First, the  $(\Delta T)_{R_o}$  for each surface is determined by the following equation:

$$q_{\min} = k_v \frac{(\Delta T)_{R_o}}{\Delta x} \quad (10)$$

where  $q_{\min}$ ,  $k_v$ , and  $\Delta x$  are the minimum heat flux determined experimentally, thermal conductivity of the vapor film, and the minimum film thickness, respectively.

Secondly, the  $(\Delta T)_{\text{hyd}}$  can be calculated by subtracting the  $(\Delta T)_{\text{Ro}}$  from the measured  $(\Delta T)_{\text{min}}$  for the copper surface. Table 4 illustrates the comparison of the roughness,  $q_{\min}$ ,  $(\Delta T)_{\text{min}}$  and  $(\Delta T)_{\text{Ro}}$  for each surface. It is seen from Table 4 that the rougher the surface, the higher the  $(\Delta T)_{\text{Ro}}$ . One can extend this analysis to estimate the minimum temperature difference,  $(\Delta T)_{\text{est}}$ , for enhanced surfaces. The procedure is to add the  $(\Delta T)_{\text{Ro}}$  value for the enhanced surface, which is calculated individually by equation (10), to the  $(\Delta T)_{\text{hyd}}$  determined to be 39.3 K, which is assumed to be constant for all surfaces. The estimated minimum temperature differences for UNB #1 and UNB #2 are 51 and 73 K, respectively, which represents 81 and 82% of the actual  $(\Delta T)_{\text{min}}$  values for two surfaces. The fact that the values of  $(\Delta T)_{\text{min}} - (\Delta T)_{\text{Ro}}$  for enhanced surfaces (42.3 and 55 K for UNB #1 and UNB #2, respectively) are greater than the assumed  $(\Delta T)_{\text{hyd}}$  for 39.3 K implies that there is another contribution to the  $\Delta T_{\text{min}}$  for the enhanced surfaces and it is believed the contribution is due to the unique vapor flow phenomena in the porous structure of the enhanced surfaces. From this analysis, it is concluded that the surface finish on plain surfaces may not play an important role on the  $(\Delta T)_{\text{min}}$  as claimed by Berenson. The surface treatment, however, greatly influences the  $(\Delta T)_{\text{min}}$  in such a favorable way that film boiling would not occur easily for the enhanced surfaces.

#### 4. CONCLUSION

Throughout the nucleate and film boiling heat transfer experiments in R-11 at 1 and 2 bar with a plain copper surface and two types of enhanced surfaces, the following points are achieved.

(1) Enhanced surfaces (UNB #1, UNB #2) show 2–3 times higher heat transfer coefficients at constant heat flux as compared to the plain copper surface in the fully developed nucleate boiling regime. Surface roughness test results indicate that rough surfaces have larger heat transfer area which is partly responsible for the heat transfer enhancements. They are also characterized by larger scale boiling hysteresis caused by larger pores and interconnecting channels.

(2) For all surfaces investigated, the superheat decreases by 15–25% as the inclination angle changes from 0° to 165° in the relatively low heat flux range, 10–40 kW m<sup>-2</sup>. Beyond this heat flux range, however, the superheat remains constant regardless of the surface orientation. The horizontally facing downward case has the lowest heat transfer coefficient due to its own typical bubble mechanism. This suggests that the upper portion of the cylindrical tank (165–180°) must

be protected well since film boiling would occur very easily at this portion.

(3) Rohsenow's nucleate boiling correlation is modified to account for the effects of the surface characteristics and orientation. For the enhanced surfaces, the exponent  $r$  is two times greater than that of the plain surface, while the coefficient  $C_{\text{sf}}$  is 1.5–2 times smaller than that of the plain surface. The present nucleate boiling data also turns out to be in good agreement with the existing experimental data in the literature. Two equations are proposed for  $r$  and  $C_{\text{sf}}$  in Rohsenow's correlation to account for their variation as a function of the surface orientation for the plain surface.

(4) The motion and stability of the vapor film on the surface are greatly influenced by surface orientation and they are responsible for the variation of film boiling data obtained for the inclined surfaces. As the stability of the film increases, the heat transfer is retarded considerably, which is well illustrated especially when the heating surface is horizontally facing downward.

(5) Berenson's prediction of the minimum temperature difference,  $(\Delta T)_{\text{min}}$ , for the plain surface facing upward is proven to be reliable within 10% deviation with respect to the present experimental data. The  $(\Delta T)_{\text{min}}$  at 1 bar in R-11 for a plain surface facing upward turns out to be 63 K. Predictions for the minimum heat flux, however, can be used only to tell the lower bound.

(6) One-dimensional heat transfer analysis is done to explain the role of surface treatment in film boiling. It turned out that the surface finish may not influence the  $(\Delta T)_{\text{min}}$  for plain surfaces. The surface treatment causing higher roughness and porosity, however, affect the  $(\Delta T)_{\text{min}}$  significantly in such a way that rough surfaces have higher minimum temperature differences. With these characteristics, the enhanced surfaces are proven to have a favorable heat transfer in film boiling since they are not apt to go over film boiling as easily as a plain surface is.

*Acknowledgment*—Funding for this work was provided by NSERC and Transport Canada. Dr D. A. Didion, Group Leader, Thermal Machinery Group, CBT, NBS, Gaithersburg, helped the first author to prepare the manuscript.

#### REFERENCES

1. R. D. Appleyard, Testing and evaluation of the EXPLOSAFE system as a method of controlling the boiling expanding vapour explosion (BLEVE), Report TP 2740, Dept. of Res. and Dev., EXPLOSAFE Div., Vulcan Industrial Packaging Ltd. (1980).
2. A. E. Bergles, J. G. Collier, J. M. Delhaye, G. H. Hewitt and F. Mayinger, *Two Phase Flow and Heat Transfer in the Power and Process Industries*, Chap. 12. Hemisphere, Washington, DC (1981).
3. R. M. Milton and C. F. Gottzmann, High efficiency hydrocarbon reboilers and condensers, paper presented at the AIChE 71st National Meeting, Dallas, Texas (Feb. 1972).

4. P. S. O'Neill, C. F. Gottzmann and J. W. Terbot, Novel heat exchanger increases cascade cycle efficiency for natural gas liquefaction, *Adv. Cryogen. Engng* **17**, 421–437 (1971).
5. K. Nishikawa, T. Ito and K. Tanaka, Enhanced heat transfer by nucleate boiling on a sintered metal layer, *Heat Transfer—Jap. Res.* **8**, 65–81 (1979).
6. S. Yilmaz, J. J. Hwalek and J. W. Westwater, Pool boiling heat transfer performance for commercial enhanced tube surfaces, ASME paper No. 80-HT-41, Orlando (July 1980).
7. P. J. Marto and V. J. Lepere, Pool boiling heat transfer from enhanced surfaces to dielectric fluids, *ASME J. Heat Transfer* **104**, 292–299 (May 1982).
8. A. E. Bergles and M. C. Chyu, Characteristics of nucleate boiling from porous metallic coating, *ASME J. Heat Transfer* **104**, 279–285 (May 1982).
9. L. A. Bromley, Heat transfer in film boiling, *Chem. Engng Prog.* **46**, 221–227 (1950).
10. Y. P. Chang, Wave theory of heat transfer in film boiling, *ASME J. Heat Transfer* **81**, 1–12 (1959).
11. N. Zuber, On the stability of boiling heat transfer, *ASME Trans.* **80**, 711–715 (1958).
12. P. J. Berenson, Film boiling heat transfer from a horizontal surface, *ASME J. Heat Transfer* **83**, 351–358 (1961).
13. P. J. Berenson, Experiments on pool boiling heat transfer, *Int. J. Heat Mass Transfer* **5**, 553–558 (1962).
14. E. R. Hosler and J. W. Westwater, Film boiling on a horizontal plate, *ARS J.* **32**, 553–558 (1962).
15. P. M. Githinji and R. H. Sabersky, Some effects of the orientation of the heating surfaces in nucleate boiling, *ASME J. Heat Transfer* **379** (1963).
16. L. T. Chen, Heat transfer to pool boiling Freon from inclined heating plate, *Lett. Heat Mass Transfer* **5**, 111–120 (1978).
17. N. Seki, S. Fukusako and K. Torikoshi, Experimental study on the effect of heating circular plate on film boiling heat transfer for fluorocarbon refrigerant R-11, *ASME J. Heat Transfer* **100**, 624–628 (1978).
18. D. S. Jung, Pool boiling heat transfer, the effects of enhanced surfaces and inclination, MScE thesis, University of New Brunswick (1984).
19. T. Fujii and H. Imura, Natural convection heat transfer from a plate with arbitrary inclination, *Int. J. Heat Mass Transfer* **15**, 755 (1972).
20. C. Corty and A. S. Foust, Surface variables in nucleate boiling, *Chem. Engng Prog. Symp. Ser.* **17**, 51 (1955).
21. K. Yamagata, F. Kirano and K. Nishikawa, Nucleate boiling of water on the horizontal heating surface, *Mem. Fac. Engng Kyushu* **15**, 98 (1955).
22. W. M. Rohsenow, A method of correlating heat transfer data for surface boiling of liquids, *ASME* **74**, 969–975 (1952).
23. N. Zuber and H. K. Forster, Bubble dynamics and boiling heat transfer, *A.I.Ch.E. Jl* **1**, 532–535 (1955).
24. Y. P. Chang and N. W. Snyder, Heat transfer in saturated boiling, ASME-AIChE Heat Transfer Conf., Storrs, Connecticut, *Chem. Engng Prog. Symp. Series* **56**, 25–38 (1960).
25. R. I. Vachon, G. H. Nix and G. E. Tanger, Evaluation of constants for the Rohsenow pool-boiling correlations, *ASME J. Heat Transfer* **90**(2), 239–247 (1968).
26. Thermodynamic properties of Freon-11 and transport properties of Freon fluorocarbons, Dupont Comp. (Inc.), Wilmington, Delaware.
27. K. Stephan and M. Abdelsalam, Heat transfer correlations for natural convection boiling, *Int. J. Heat Mass Transfer* **23**, 73–87 (1980).
28. K. Akagawa, T. Sakaguchi and T. Fujii, Influence of fouling on boiling heat transfer to organic coolants, Fifth International Heat Transfer Conference, Japan, Vol. 4, p. 25 (1974).

#### EFFETS DES SURFACES AMELIOREES OU DE L'ORIENTATION DES SURFACES SUR L'EBULLITION NUCLEE OU EN FILM POUR R-11

**Résumé**—On étudie l'ébullition du R-11 en réservoir en fonction de la caractérisation de la surface et de son orientation. Deux surfaces spécialement recouvertes de métal (UNB # 1, UNB # 2) et une surface plane de cuivre sont soumises à des flux de chaleur allant jusqu'à  $180 \text{ kW m}^{-2}$ , avec des orientations variant depuis l'horizontale face supérieure ( $0^\circ$ ), à l'horizontale face inférieure ( $180^\circ$ ) en passant par la verticale ( $90^\circ$ ). Les courbes d'ébullition nucléée montrent une hystérésis et les surfaces améliorées transfèrent 2–3 fois plus qu'une surface lisse. L'équation de Rohsenow pour l'ébullition nucléée est utilisée pour représenter les données et elle est modifiée pour tenir compte des effets de caractérisation de surface et d'orientation. Dans l'ébullition en film, les surfaces améliorées révèlent aussi de meilleures caractéristiques de transfert thermique et le rôle de l'orientation sur le mouvement et la stabilité du film de vapeur est clarifiée.

#### EINFLUSS VON KÜNSTLICHER VERGRÖßERUNG EINER OBERFLÄCHE UND DEREN ORIENTIERUNG AUF DEN WÄRMEÜBERGANG BEIM BLASEN- UND FILMSIEDEN VON R-11

**Zusammenfassung**—Es wird über eine Untersuchung der Abhängigkeit des Wärmeübergangs beim Behältersieden von R-11 von den Eigenschaften und der Orientierung der Oberfläche berichtet. Zwei speziell präparierte metallbeschichtete Oberflächen (UNB # 1, UNB # 2) und eine ebene Kupferoberfläche wurden mit Wärmestromdichten bis zu  $180 \text{ kW m}^{-2}$  beaufschlagt. Die Oberflächenlage wurde von horizontal nach oben gerichtet ( $0^\circ$ ) über vertikal ( $90^\circ$ ) bis zu horizontal nach unten gerichtet ( $180^\circ$ ) variiert. Die gemessenen Kurven beim Blasensieden zeigen eine deutliche Siedehysterese. Bei den künstlich vergrößerten Oberflächen wurden Wärmeübergangskoeffizienten ermittelt, die zwei- bis dreimal höher waren als diejenigen an der ebenen Oberfläche. Die Rohsenow-Gleichung für Blasensieden wurde zur Korrelation der Meßwerte benutzt. Um die Einflüsse der Beschaffenheit und der Orientierung der Oberfläche zu berücksichtigen, wurde die Gleichung modifiziert. Beim Filmsieden ergibt sich für die künstlich vergrößerten Oberflächen ebenfalls eine bessere Wärmeübertragungscharakteristik als für die ebene Oberfläche. Der Einfluß der Oberflächenorientierung auf Bewegung und Stabilität des Dampffilms wurde geklärt.

**ВЛИЯНИЕ АРМИРОВАНИЯ ПОВЕРХНОСТЕЙ И ИХ ОРИЕНТАЦИИ НА ТЕПЛОБМЕН ПРИ ПУЗЫРЬКОВОМ И ПЛЕНОЧНОМ КИПЕНИИ R-11**

**Аннотация**—Теплообмен при кипении R-11 в большом объеме изучен в зависимости от качества и ориентации поверхности. Две специально обработанные поверхности с металлическим покрытием (UNB #1, UNB #2) и одна плоская медная поверхность подвергались воздействию тепловых потоков до  $180 \text{ кВт/м}^2$ . В этом случае ориентация поверхностей изменялась от горизонтальной обращенной вверх ( $0^\circ$ ) до вертикальной ( $90^\circ$ ) и горизонтальной обращенной вниз ( $180^\circ$ ). Полученные кривые для пузырькового кипения указывают на заметный гистерезис кипения, а армированные поверхности интенсифицируют теплообмен в 2–3 раза по сравнению с неармированными. Для обобщения данных используется уравнение Розенау для пузырькового кипения, которое модифицируется с учетом влияния качества и ориентации поверхности. При пленочном кипении характеристики теплообмена армированных поверхностей лучше. Уточняется влияние ориентации на движение и устойчивость пленки пара.